Journal of Thermal Science Vol.30, No.4 (2021) 1302−1317

https://doi.org/10.1007/s11630-021-1478-4 **Article ID: 1003-2169(2021)04-1302-16**

Numerical Study on Flow Heat Transfer Characteristics of Horizontal Tube Falling-Film Evaporator

XU Bo[1], JIANG Chun[1], CHEN Zhenqian[1,2,3*]

1. School of Energy and Environment, Southeast University, Nanjing 210096, China
2. Jiangsu Provincial Key Laboratory of Solar Energy Science and Technology, School of Energy and Environment, Southeast University, Nanjing 210096, China
3. Key Laboratory of Energy Thermal Conversion and Control of Ministry of Education, School of Energy and Environment, Southeast University, Nanjing 210096, China

Abstract: As an efficient and energy-saving heat exchange technology, horizontal tube falling film evaporation has a great application prospect in refrigeration and air conditioning. The three-dimensional models of falling film flow evaporation outside horizontal single tube and inside evaporator were established, and the accuracy of flow and heat transfer simulation process was verified by comparison. For horizontal single tube, the results showed that total heat transfer coefficient was low and increased with larger spray density and evaporation temperature. The thickness of liquid film outside tube decreased gradually with the increase of tube diameter, and the total heat transfer coefficient of small tube diameter was significantly greater than that of the large tube diameter. The total heat transfer coefficient presented an increasing trend with larger liquid distribution height and density. In addition, the fluctuation of tube axial liquid film thickness distribution decreased with larger liquid distribution density. For evaporator, the results indicated that part of liquid refrigerant was carried into the vapor outlet. The temperature of tube wall and fluid presented a gradually rising trend in vertical downward direction, while tube wall temperature within the same horizontal and transverse row had little difference. The high-temperature zone on the outer wall of heat exchange tube moved towards the inlet and gradually decreased, and the outlet temperature of water in the tube also gradually decreased with the increase of refrigerant spray density. The local heat transfer coefficient of heat exchanger tube in the vertical direction presented a downward trend which was more obvious with the smaller spray density and it was obviously higher located in the middle of upper tube row and both sides of lower tube row for horizontal tube rows.

Keywords: horizontal single tube, evaporator, falling film, numerical simulation, heat transfer

1. Introduction

Air conditioning, refrigeration and heating account for more than 65% of building energy consumption in our country and the energy consumption level of large public buildings is generally high [1]. As a big energy consumer, how to improve the efficiency of energy utilization and reduce pollution emissions is one of the most important

Received: May 09, 2020 AE: FAN Liwu Corresponding author: CHEN Zhenqian E-mail: zqchen@seu.edu.cn

issues at present [2]. Horizontal tube falling-film evaporative cooling technology has been widely used in air conditioning systems and various industries as one of the energy efficient utilization technologies and has attracted more and more scholars' attention [3]. Therefore, it is of great significance to study the flow and heat transfer characteristics of falling film evaporation in horizontal tube to improve the efficiency of evaporator and energy efficiency.

Most of numerical simulation studies on the falling film flow outside the tube simplified the actual physical model into a two-dimensional model, ignoring the liquid axial spreading flow [4–10]. Wang et al. [4] and He et al. [5] established a two-dimensional model of falling film flow outside the horizontal tube through numerical simulation method and explored the influence of factors such as velocity, tube spacing and pore diameter on the liquid film thickness distribution outside the tube with refrigerant R134A. Qiu et al. [6] carried out a two-dimensional numerical simulation of liquid film distribution on the horizontal tube surface by using VOF method. The results showed that the flow of liquid film along the horizontal tube circumferential direction can be divided into a transient process and then a steady-state process. Yang et al. [7] studied the influencing factors of liquid flow outside the horizontal falling-film evaporator tube and optimized the tube bundle structure by observing the liquid film flow state and calculating the liquid film thickness under different conditions. The microcosmic mechanism of heat transfer in horizontal tube falling film flow was investigated by Yang et al. [8]. It was believed that there was a laminar layer in the transition region of laminar flow and micro-turbulence, and it was the main thermal resistance of heat transfer in the film. In the tube outer circumferential 5°, the circulating reflux explains the region near the microscopic mechanism of heat transfer reinforcement. What's more, the boundary condition of tube wall was set as constant wall temperature or constant heat flux for most of current numerical simulation to simplify calculation process, while the problem was that it can't reflect the heat transfer law comprehensively and objectively. Yang et al. [9] set the tube wall as constant wall temperature condition to obtain the distribution characteristics of thermal parameters such as liquid film thickness, liquid film flow velocity and heat transfer coefficient in the liquid film. Jafar et al. [10] established a two-dimensional falling-film flow evaporation model for three-row tube and treated the inner wall as the boundary of constant heat flux to analyze the influence of different spray density and tube diameter on the heat transfer coefficient outside the tube. Zhou et al. [11] set the inner wall surface as the boundary of constant heat flux. The results indicated that "dry up" area would be formed at the tube bottom and it would increase with larger spray density. In addition, the overall heat transfer coefficient was mainly determined by the heat transfer coefficient of film inside tube in the horizontal tube axial direction. The increase of spray density had a significant effect on the heat transfer coefficient of film outside tube, while it has no obvious effect on the heat transfer coefficient of film inside tube.

At present, a large number of researches mainly focus on single heat exchange tube. Gstoehl et al. [12] and He et al. [13] adopting the method of laser induced fluorescence to measure liquid film thickness outside the horizontal single tube. The fluorescent substances were added in working medium to enhance measurement accuracy and the high-definition cameras were used to capture the distribution and change of liquid film. The results concluded that the liquid film thickness in the upper tube was greater than the lower half of tube and the minimum thickness of liquid film in the circular tube was within the range of 90° to 120° circumferential angle. Xu et al. [14, 15] used intelligent film thickness micrometer to measure the liquid film thickness outside the heat exchange tube with diameter of 20 mm, 25 mm, 30 mm and 40 mm respectively. It was concluded that the probability distribution of the outer liquid film thickness increased with the larger liquid load, and it decreased first and then increased along the circumference of tube. Parken et al. [16–18] carried out an experimental study on the effect of tube diameter on the evaporative heat transfer coefficient of horizontal falling film. The results showed that the heat transfer coefficient increased with the decrease of tube diameter because the fluctuation of liquid film surface became more severe with the decrease of tube diameter, enhancing the convection heat transfer. In practical engineering application, it often appeared in the form of transposition tube bundle and the research of single heat exchange tube can't bring intuitive results and more convincing basis for practical engineering.

In this paper, falling film flow evaporation of a complete evaporator was studied. The 3D numerical models of refrigerant (R410A) falling film flow evaporation outside the horizontal single tube and inside the evaporator were established, using the flow coupling heat transfer boundary between tube inside and outside. The film thickness and heat transfer coefficient were analyzed. The 3D flow process and heat transfer characteristics were simulated and the influence rule of different parameters on the evaporation of falling film flow outside the horizontal tube was explored.

2. Models and Methods

2.1 Falling-film evaporation of horizontal single tube

2.1.1 Model

In this paper, refrigerant (R410A) and coolant (water)

were used in the horizontal single tube outer falling-film evaporation. In order to ensure the accuracy of numerical simulation results, the physical characteristics of working medium changing with temperature were considered. In FLUENT software, physical properties of fluid working medium under different temperature conditions were set by piecewise linear method. According to the design conditions of comparison experiment [19], the corresponding physical model of numerical simulation was established with size of 90 mm×39 mm×39 mm, shown in Fig. 1. The refrigerant layout height was H and refrigerant layout hole diameter was d=2 mm. The outside diameter of heat exchange tube was D and thickness of tube wall was ε=1 mm. The horizontal distance between center of refrigerant layout hole and axis of heat exchange tube was S=4 mm. R410A fell from refrigerant layout height to evaporation tube top at spray density of level 2 $kg \cdot m^{-1} \cdot s^{-1}$. The liquid film flowed downward under the action of gravity, viscous force and surface tension, and continuously evaporated by heat.

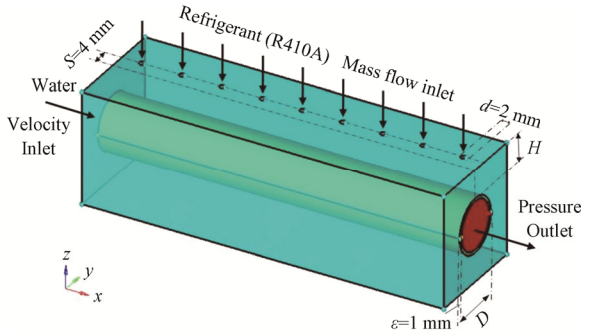

Fig. 1 Model of falling-film evaporation of horizontal single tube

2.1.2 Boundary conditions and grid partition

Liquid film Reynolds number corresponding to falling-film flow evaporation outside the horizontal tube generally ranged from 800 to 4000 [20], and the variation range of liquid film Reynolds number in this paper was also within this range. The boundary conditions for the calculated area were set as follows: the refrigerant layout hole inlet was set as mass-flow-inlet; the upper and lower side surfaces were respectively the pressure-inlet and pressure-outlet boundaries, and the gauge pressure of inlet was 0 Pa. Adiabatic wall boundary conditions were set at the left and right walls, and no slip boundary conditions were used for wall velocity; to avoid the influence of front and rear boundaries on circumferential fluid flow, front and rear boundaries were set as symmetry boundaries; the inner and outer walls of horizontal heat exchange tube were coupled boundary conditions; the inlet of coolant water was set as velocity inlet with v_{in}=1.5 m/s [21] and the outlet was set as the pressure-outlet. Time step was 5×10^{-4} s.

In order to ensure the quality and efficiency of mesh generation and the accuracy of numerical calculation, hypermesh method for mesh generation was used. Hexahedral structured grid was used inside the tube and near the wall, and tetrahedral unstructured grid was used in other areas because structural parameters needed to be changed according to different research conditions. As the gas-liquid two-phase flow required a high quality of grid, the near-wall area of heat exchange tube was intensified to ensure the computational accuracy of falling-film flow area.

2.1.3 Calculation methods

VOF algorithm [22] was adopted to dynamically track the free boundary flow of gas-liquid phase, accounting for mass transfer between two phases. The volume fraction of phase in the VOF model was taken as a variable and the sum of each phase volume fraction was 1. The numerical calculation of phase change problem required the determination of evaporation and heat source term related to phase change. Therefore, the Lee model [23, 24] based on physical and mechanical model was adopted to define the mass and energy transfer between different phases. The surface tension model was applied to improve the accuracy of simulation. Continuous Surface Force (CSF) model [25] was selected as the surface tension model and realized by adding source terms into the momentum equation. To understand the origin of the source term, consider the special case where the surface tension is constant along the surface, and where only the forces normal to the interface are considered.

The solution was set as follows: (1) the calculation area was a three-dimensional rectangular coordinate system and the flow field was a non-steady state simulation; (2) assuming that the working medium was a continuous and incompressible fluid, the shear force and pressure gradient between gas-liquid interface were ignored and they were in thermodynamic equilibrium state; (3) PISO algorithm was adopted in pressure velocity coupling and PRESTO! algorithm discretized the pressure term; (4) the gas-liquid interface was captured by Modified-HRIC method with both speed and precision. The energy and momentum equations were discretized by second-order upwind format; (5) influences of gravity and surface tension were taken into account in the flow.

2.2 Horizontal tube falling-film evaporator

2.2.1 Model

Based on the simulation analysis of horizontal single tube outer falling-film evaporation, a three-dimensional physical model of horizontal tube falling-film evaporator

was established. In order to truly reflect flow heat transfer process of evaporator, the coupling heat transfer between coolant water in tube side and refrigerant R410A in shell side through the wall surface of heat transfer tube was considered. The tube wall thickness of heat exchange tube was not drawn in the model due to the relatively large size of evaporator. The refrigerant layout hole was simplified to a porous liquid dispenser plate and the inlet of liquid pipeline didn't draw separately. The three-dimensional simplified model included heat exchange tube bundle, porous liquid dispenser plate, shell, water inlet and outlet, refrigerant liquid outlet and refrigerant steam outlet, depicted in Fig. 2. Based on the analysis of evaporative flow and heat transfer characteristics on the external falling-film flow of a horizontal single tube, the diameter of heat exchange tube was D=10 mm; the height of liquid dispenser plate was H=10 mm, and the arrangement density of liquid distribution hole was 11 (the axial spacing between adjacent liquid distribution holes was 10 mm). The liquid dispenser plate was directly on the tube axis. The specific structural parameters were described in Table 1.

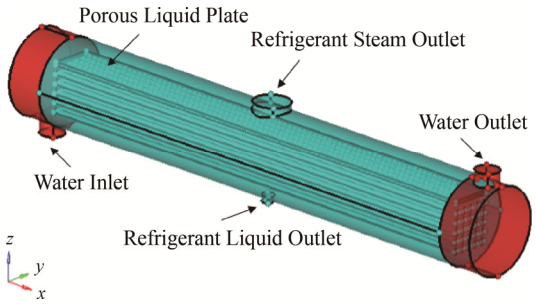

Fig. 2 Model of horizontal tube falling-film evaporator

Table 1 Structural parameters of horizontal tube falling-film evaporator

Parameters	Unit	Values
Shell inner diameter	mm	120
Outside diameter of heat exchange tube	mm	10
Number of heat exchange tubes	–	25
Effective length of heat exchange tube	mm	800
Arrangement of heat exchange tube	–	Square layout
Center distance of heat exchange tube	mm	15
Shell side inlet and outlet inner diameter	mm	40
Inner diameter of refrigerant liquid outlet	mm	60
Inner diameter of refrigerant steam outlet	mm	20
Refrigerant layout hole diameter	mm	2

2.2.2 Calculation methods and boundary conditions

The boundary conditions of the model were set as follows: the inlet of shell refrigerant (inlet of porous liquid dispenser plate) was set as mass-flow-inlet with inlet temperature of 279.15 K. The shell refrigerant outlet was divided into two parts, both of which were pressure-outlet boundaries. The refrigerant steam flowed away from upper outlet and the refrigerant liquid flowed away from lower outlet. Inlet of coolant water in tube was set as mass-flow-inlet with temperature of 285.15 K and the outlet was set to pressure-outlet boundary condition. The wall surface of heat exchange tube was coupled with no permeability and no slip with wall thickness of 1 mm. The other wall boundary conditions were all set as no permeability and no slip adiabatic wall boundary.

The initial settings were described as followed at time of 0: shell side was filled with R410A gas; coolant water filled the tube side at the set initial velocity and the liquid phase volume fraction at the inlet of liquid distribution hole was 1. The solutions of first four items were the same as those in Section 2.1.3. The other two items were set as the flow process considering the influence of gravity at 9.81 m/s^2 and ignoring the external heat dissipation of evaporator shell outer wall.

In the process of iterative calculation, the residual values of continuity parameters and energy parameters were control within the scope of 10^{-4} and 10^{-7} magnitude separately. The stability of residual error curve stood for finish of iterative calculation with reference to many similar simulation studies due to the relatively complex flow and heat transfer process in falling-film evaporator.

2.3 Grid independence and time step independence

Grid independence was studied and liquid film thickness at the model center changing with circumferential angle depicted in Fig. 3 when liquid film Reynolds number was 1000. In order to investigate the dependence of grid, grid numbers were selected as 225 817, 632 551 and 1 095 820 to simulate the same boundary conditions of falling film flow process. When the number of grids reached 632 551, the relative error was within 5% and the density of grids had little impact on the simulation results. Therefore, the grid model with the number of 632 551 was selected for subsequent calculation.

In the process of numerical simulation, the time step setting in unsteady state calculation has an important influence on the final calculation result. If the time step size is too large, it would affect the system stability and the calculation convergence, leading to the final divergence of calculation. At the same time, it would lead to unacceptable errors and deviation from the real results. The liquid film spreading from the top of horizontal pipe to the complete state was a transient process with time variation, causing the influence of time step on calculation results. Time step independence was studied

and liquid film thickness at the circumferential angle of 120° with time step was depicted in Fig. 4. It can be found that when the time step was less than 5×10^{-4} s, the change range of liquid film thickness was small and tended to be stable. However, when the time step was larger than 5×10^{-4} s, the liquid film thickness increased substantially with larger time step, causing the huge calculation errors. It can be considered that the calculated results had time step independence when time step was less than 5×10^{-4} s.

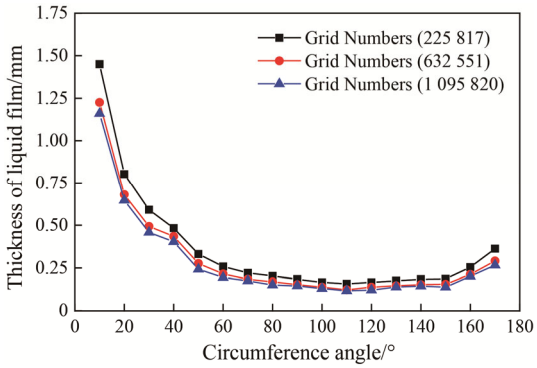

Fig. 3 Grid independence

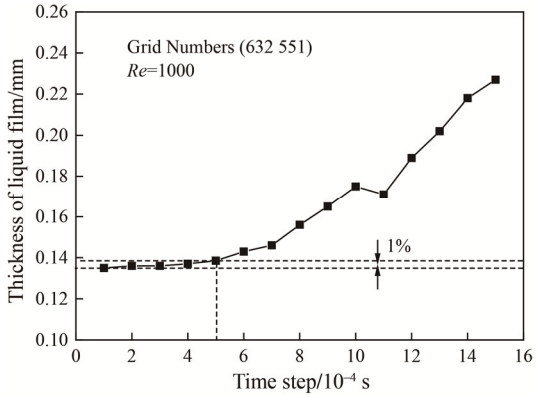

Fig. 4 Time step independence

2.4 Validation of model and methods

2.4.1 Dimensionless heat transfer coefficient

The dimensionless heat transfer coefficient during falling film evaporation was calculated as follows:

$$h^+ = h\left(\frac{\mu^2}{g\rho^2\lambda^3}\right)^{\frac{2}{3}} \tag{1}$$

The relative parameters between simulation and experiment were set in Table 2 and the results were shown in Fig. 5. The numerical simulation results of this paper were slightly higher than the experimental data, which was due to the relative ideal assumptions in the process of numerical simulation. The heat loss in the experiment was not considered in simulation and the tube diameter and wall thickness were rounded considering the meshing, which were smaller than experimental conditions. Therefore, the proportion of its thermal development area was larger, causing a certain increase in heat transfer coefficient. However, the overall relative error between simulation and experiment was less than 10%. What's more, the variation of dimensionless heat transfer coefficient of simulation and experiment with Reynolds number was consistent, indicating the settings of calculation method and condition in this model were reasonable and reliable.

The physical properties of fluid working medium under different temperature conditions were set by piecewise linear method in the paper. Compared with the simulation method of simplifying physical properties of fluid working medium by assuming constants, it was found the results of temperature dependent fluid properties were closer to experimental data and it was more accurate. The *Re* was closely related to dynamic viscosity, which was changed by different temperature. Therefore, the application of temperature dependent fluid properties method could improve the accuracy and authenticity of simulation result.

Table 2 Relative parameters between simulation and experiment

	Saturation temperature /K	Saturation pressure /MPa	Diameter /mm	Tube wall thickness /mm
Simulation	279.15	0.9653	19.00	1.00
Experiment [26]	279.15	0.9653	19.05	1.15

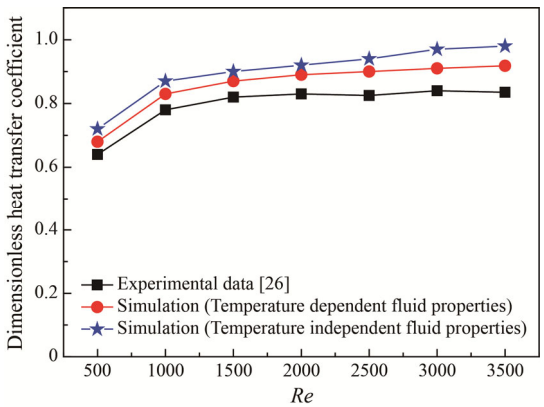

Fig. 5 Comparison of simulation results and experiment on dimensionless heat transfer coefficient

2.4.2 The flow pattern of liquid film outside tube

The flow process of falling film outside the horizontal tube referred to the process in which the liquid flowed out of liquid distribution hole, collided with upper side of tube, spread along the circumferential and axial

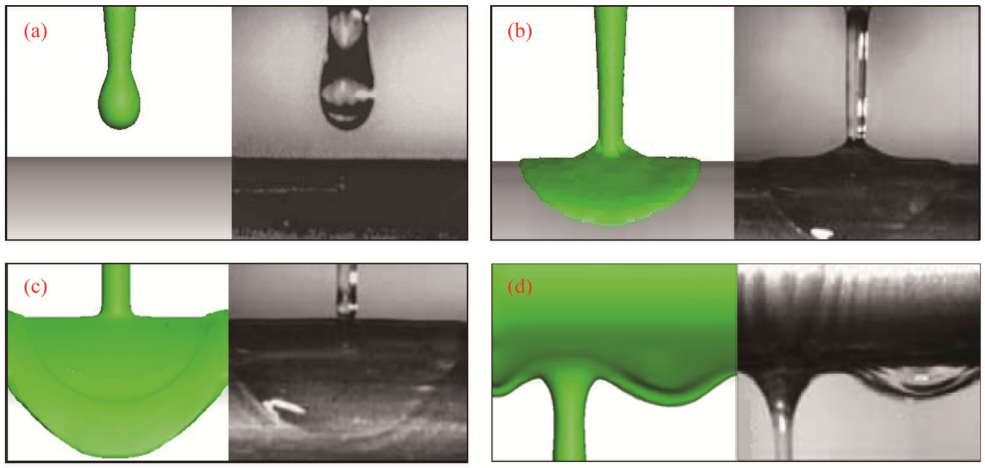

Fig. 6 Comparison of numerical simulation results and experiment. (a), (b), (c) [29] and (d) [27]

directions and finally separated from the bottom of heat exchange tube. Although the description of this process was complex, the process for the falling film flow in a single tube was generally only 0.3 s–0.8 s. It was more efficient and convenient to simulate and capture the dynamic process through numerical simulation because it was very difficult to capture such a short liquid flow process. In order to compare and verify the actual process of falling film flow of liquid in a horizontal single tube, the experimental results of Killion and Garimella [27–29] were selected as the reference, shown in Fig. 6. At the initial stage of falling film flow, the liquid film was approximately inverted trapezoid on the outer wall of heat exchange tube and local accumulation of liquid film also occurred between the liquid columns at the heat exchange tube bottom. Because the working medium, liquid dispenser height and spray density used in the simulation were not completely consistent with the comparison experiment, there were still some differences in flow morphology. For example, slight fluctuations appeared on the surface of liquid film flow in the experimental observation, which were not well presented in the numerical simulation. It was mainly because smooth tubes were used for heat exchange in simulation to build model conveniently, neglecting the effect of surface quality like roughness and production defects on liquid film flow. The surface quality in experiment leaded the fluctuations of liquid film flow surface. At the same time, liquid film along the axial spreading margin uplift formed local accumulation of liquid film while there was no phenomenon in the corresponding experimental observation in Fig. 6(c). It was mainly because the multiple liquid columns were formed by liquid dispenser hole in simulation model and the local accumulation of liquid were formed by the axial spreading of adjacent liquid column. However, the flow pattern of outside tube liquid film obtained by numerical simulation was generally in good agreement with the observed results of relevant experiments. Therefore, it can be considered that the flow characteristics and film-forming laws presented by the three-dimensional numerical simulation of falling film flow outside the tube in this paper were reliable.

3. Results and Discussion

3.1 Falling-film evaporation of horizontal single tube

3.1.1 The “dry up” area formed by liquid film rupture

The optimal state of horizontal falling film flow heat transfer was that the refrigerant liquid can flow and spread into a complete and uniform liquid film on outer wall of each heat exchange tube. If the thickness of outer liquid film was too thick, it would increase the resistance of heat transfer. If the thickness of outer liquid film was too thin, it would be easily affected by the heat flow density, heat exchanger structure or other factors to form a “dry up” area outside the tube, greatly reducing the heat transfer effect of falling film flow evaporation. In the process of outside horizontal tube falling film flow, the liquid was affected by gravity, surface tension of gas liquid interface and viscous force on the tube wall surface. The gravity made the liquid flow outside the tube become a film, and liquid film surface tended to be unstable due to the capillary pressure caused by surface tension. The direction of capillary pressure was opposite to flow direction and it made a retardation effect on liquid flow.

Liquid film form of outside tube falling film under different Reynolds number was shown in Fig. 7 and the ratio of “dry up” area to total tube falling film area with different *Re* was shown in Fig. 8. For *Re*=1500, liquid spreading along the axial and circumferential heat exchange tube formed a continuous and complete liquid film and no “dry up” area appeared. In addition, the

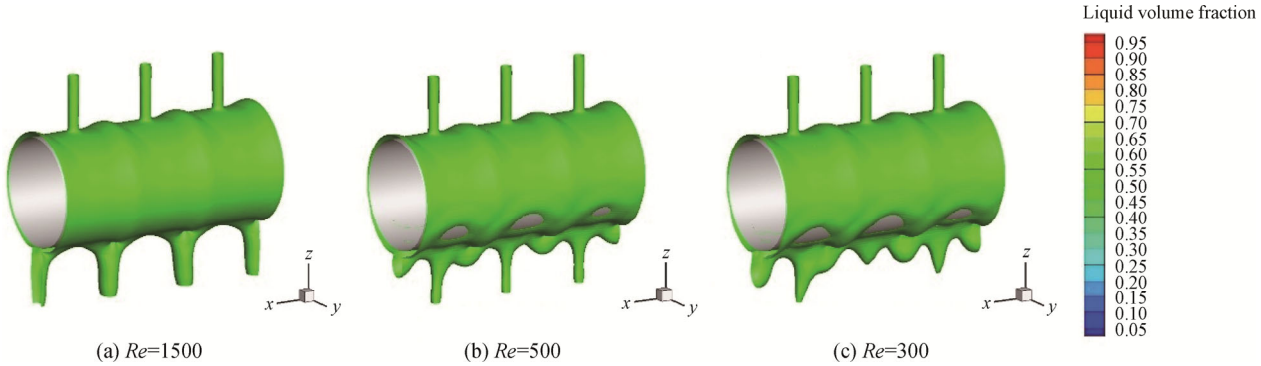

(a) *Re*=1500 (b) *Re*=500 (c) *Re*=300

Fig. 7 The "dry up" area formed by liquid film rupture

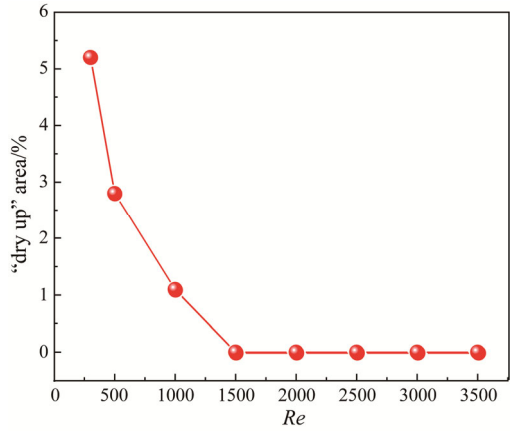

Fig. 8 The ratio of "dry up" area to total tube falling film area with different *Re*

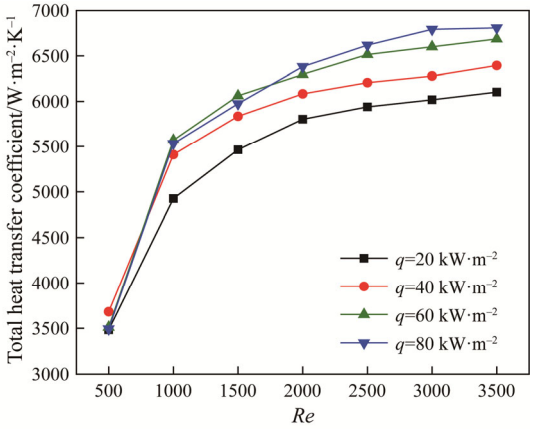

Fig. 9 Effects of spray density and heat flux density on total heat transfer coefficient

liquid leaving from the tube formed a new column below the wave appearing in the middle of the upper liquid column due to the large flow flux. When the refrigerant spray density decreased to corresponding *Re*=500, the fluctuation of outside tube liquid film and capillary pressure increased, while the flow velocity on the liquid film surface decreased. At this time, the slight interference would easily lead to the formation of stagnation point in the place of thin liquid film or low flow rate, and the local "dry up" area appeared at outside tube liquid film. When *Re*=300, the edge of "dry up" area would shrink outward to further expand its area, forming a stable and permanent "dry up" area. What's more, a stable columnar flow couldn't be formed at the bottom of heat exchange tube.

3.1.2 Effects of spray density and heat flux density on heat transfer in falling film flow

The total heat transfer coefficient of falling film evaporation was calculated with the spray density corresponding to the liquid film Reynolds number within a range of 500–3500 and the heat flow density (q) between 20 kW/m^2 and 80 kW/m^2, depicted in Fig. 9. When the refrigerant spray density was small, the total heat transfer coefficient was low and it increased significantly with the larger spray density. When the spray density corresponding to the liquid film Reynolds number increased to 2000, the increase amplitude of total heat transfer coefficient gradually decreased and it finally tended to be stable. Two reasons were described as followed. On the one hand, the flow velocity of liquid outside the tube increased with larger spray density, enhancing the disturbance of liquid film and strengthening the heat transfer effect. On the other hand, there was a local "dry up" area on outer tube wall where the refrigerant was not fully spread and covered with the small spray density. With the increase of spray density, the liquid film coverage and disturbance increased gradually, leading the improvement of heat transfer coefficient. When the spray density continued to increase, although the higher refrigerant flow rate would increase the liquid film disturbance, the liquid film thickness covered by flow outside the tube would also increase. The increase of liquid film thickness would make the increase of liquid film thermal resistance, which was not conducive to heat transfer and prevented the further improvement of heat transfer coefficient. In addition, the results obtained by other scholars indicated that when the

spray density continued to increase to a large extent, the heat transfer coefficient would also decrease to a certain extent, which was because the inhibition of heat transfer effect brought by thickening of liquid film became more obvious [30]. Therefore, it was of great significance to select the proper spray density for enhancing the falling film evaporation heat transfer.

As can be seen from the figure, the total heat transfer coefficient of outside tube falling film evaporation increased with the improvement of heat flux density at a larger spray density. It was mainly because the increase of heat flux density would raise the degree of superheat on the tube surface, leading the increase of gasification core quantity on heat exchange tube wall. The continuously produce of gasification core would further increase disturbance to the liquid film flow. However, such a pattern was not completely presented at the small spray density. At this time, the refrigerant evaporation would increase with larger heat flux density, leading the appearance of local "dry up" area and decreasing the heat transfer effect.

3.1.3 Effect of evaporation temperature on heat transfer in falling film flow

The main mechanism of evaporation temperature affecting heat transfer coefficient is that the change of evaporation temperature would change the physical properties of fluid working medium, such as gas-liquid phase density, dynamic viscosity, thermal conductivity and surface tension and have an impact on falling film flow and heat transfer. The total heat transfer coefficient of outer falling-film evaporation at Re=500 to 3500 and evaporation temperature of 276.15 K, 279.15 K, 282.15 K and 285.15 K was calculated respectively, described in Fig. 10. The total heat transfer coefficient of falling film evaporation increased with the larger evaporation temperature. Comparing with the total heat transfer coefficient of evaporation temperature at 276.15 K, the total heat transfer coefficient increased by 8.46%, 19.32% and 23.53% at evaporation temperature of 279.15 K, 282.15 K and 285.15 K respectively. The three reasons for this phenomenon were as followed. The dynamic viscosity of refrigerant decreased with the increase of evaporation temperature. The viscosity decreased by 10.54% when evaporation temperature increased from 276.15 K to 285.15 K. This directly leaded to the increase of flow velocity and the decrease of liquid film thickness outside the tube, enhancing the disturbance of liquid film flow outside the tube. In addition, the surface tension of refrigerant gas-liquid phase also decreased correspondingly with larger evaporation temperature, leading the reduction of inhibition effect of surface tension on the liquid film fluctuation and making the fluctuation of liquid film flow more obvious. Finally, the thermal conductivity of refrigerant increased with the larger evaporation temperature, enhancing the heat transfer in the liquid film. The above three factors together promoted the total heat transfer coefficient of falling film evaporation to increase with larger evaporation temperature. In actual refrigeration system, the evaporation temperature can be adjusted by changing evaporation pressure in the evaporator. With the increase of evaporation pressure, the corresponding evaporation temperature would also increase. Therefore, appropriate evaporation temperature should be selected in the actual engineering application to match the working condition and control the cost.

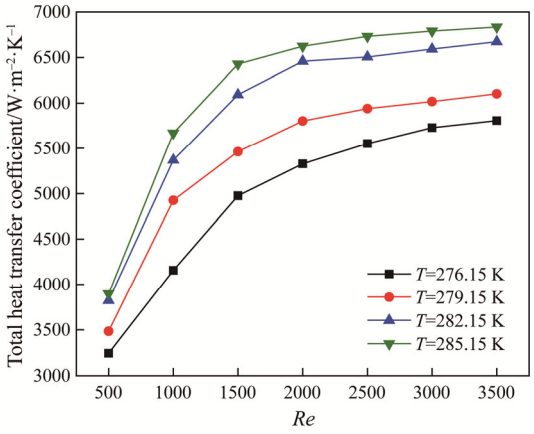

Fig. 10 Effects of evaporation temperature on total heat transfer coefficient

3.1.4 Effects of different structural parameters on heat transfer in falling film flow

3.1.4.1 Tube diameter

At present, the experimental studies of influence of tube diameter on the heat transfer of falling film flow were relatively few. It was because the adjustment of tube diameter in the experiment would increase the equipment cost and experimental cycle. In this paper, the circumferential liquid film thickness and the total heat transfer coefficient of tube central section at Re=500–3500 and tube diameter (D) of 10 mm, 16 mm, 19 mm and 25 mm were depicted in Fig. 11 and Fig. 12. As can be seen from Fig. 11, the liquid film thickness outside the tube decreased gradually with the increase of tube diameter. It was mainly because the improvement of tube diameter would lead to less liquid distribution on the tube outer wall at a constant spray density. A longer tube circumference was conducive to the "stretching" of liquid film, thus making the liquid film thinner.

As can be seen from Fig. 12, the total heat transfer coefficient of small tube diameter was significantly greater than that of large tube diameter within the range of Re=500 to 2500, especially at a lower spray density. Due to the disturbance generated by impact, the local

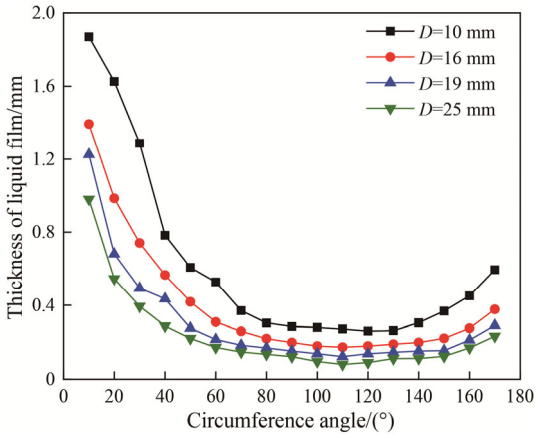

Fig. 11 Circumferential distribution of liquid film thickness with different diameters at *Re*=1000

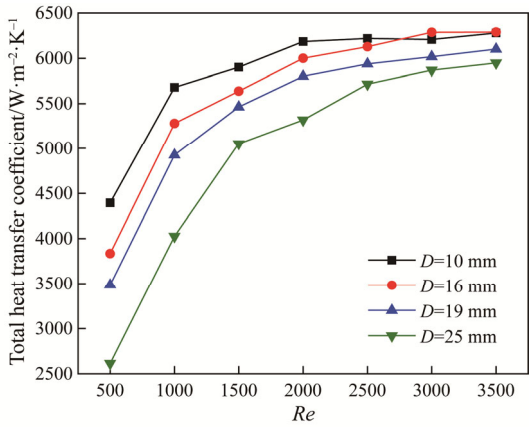

Fig. 12 Effects of tube diameters on total heat transfer coefficient

heat transfer coefficient of upper tube was largest and it gradually decreased along the tube circumference. Therefore, the heat exchange tube of small diameter can gain greater refrigerant impact area of strong heat transfer effect. At the same time, the smaller tube diameter was conducive to the spread of the refrigerant film on the outer tube wall, while the heat exchange tube with larger tube diameter was more prone to the "dry up" area of refrigerant outside the tube under the same spray density, leading the decrease of heat transfer effect. It was important to note that when liquid film Reynolds number reached 2500, the effect of diameter on total heat transfer coefficient decreased gradually with the increased Reynolds number. What's more, the heat transfer of heat exchange tube at 16 mm tube diameter was slightly better than 10 mm diameter tube, because the emergence of "dry up" area could be avoided when the tube outer refrigerant spray density was large enough. With the increase of spray density, liquid film thickness of small diameter tube and thermal resistance of heat transfer film was also bigger, leading the offset of enhancement of heat transfer in the small diameter by a certain degree. Therefore, the heat exchange tube with smaller diameter can be selected as far as possible according to the actual conditions at the small working medium spray, while it need not be pursued excessively at the enough large working medium flow in the engineering design.

3.1.4.2 Refrigerant layout height

The influence of tube spacing and bundle arrangement on the flow and heat transfer outside the tube was studied by many scholars. In essence, it was the influence of refrigerant liquid initial velocity in the falling film flow outside the heat exchange tube on the heat transfer effect causing by the difference in liquid distribution height. The variations of thickness distribution of circumferential liquid film and total heat transfer coefficient with different liquid distribution height (*H*) of 6 mm, 10 mm, 14 mm and 18 mm were depicted in Fig. 13 and Fig. 14. It can be seen that the circumferential distribution of liquid film outside the tube presented a decreasing trend on the whole and the change of liquid film thickness in the upper half of tube was larger than that in the lower half with the increase of liquid distribution height. The principal causes of this phenomenon were the initial velocity increased with the larger liquid distribution height, strengthening the disturbance of liquid film, promoting the liquid spread and flow in the tube axial and leading to the thinning of circumferential liquid film thickness. When the liquid flowed to the lower half of tube, liquid film flow was relatively steady and it was rarely affected by the disturbance of upper half impact area. Therefore, the film thickness change in lower half of tube was not big. When the liquid distribution height was 18 mm, the liquid film thickness in the upper half of tube showed a "jump" rise because of the liquid film fluctuation caused by large liquid impact velocity.

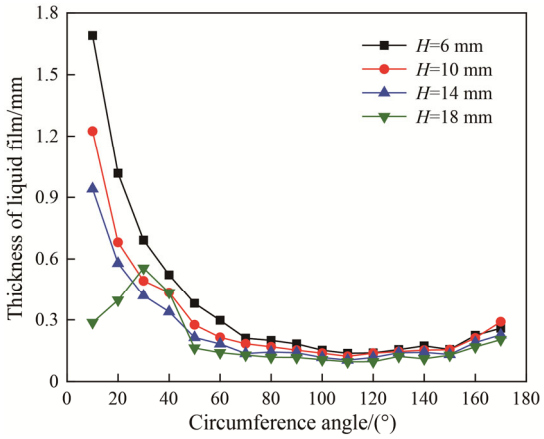

Fig. 13 Circumferential distribution of liquid film thickness with different refrigerant layout height at *Re*=1000

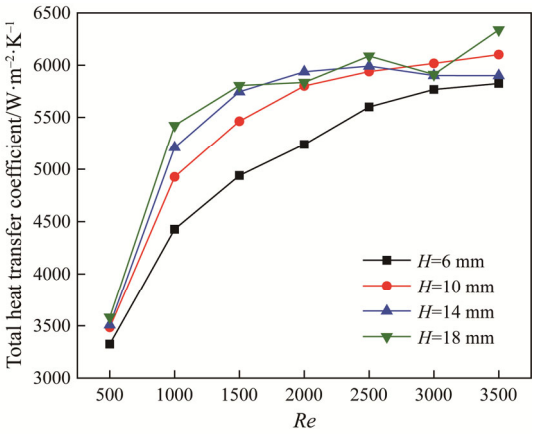

Fig. 14 Effects of refrigerant layout height on total heat transfer coefficient

The total heat transfer coefficient showed an increasing trend with the larger liquid distribution height at the small Reynolds number, because the refrigerant liquid had a greater impact on the heat exchange tube and the overall flow velocity and fluctuation of liquid film were more obvious with the increase of liquid distribution height. Especially when the liquid distribution height increased from 6 mm to 10 mm, the effect on the increase of heat transfer coefficient was obvious. The total heat transfer coefficient and liquid film distribution fluctuated at H=18 mm with the further increase of Reynolds number. This was because the increase of liquid distribution height would cause the droplet splashing and flow instability, affecting the heat transfer.

3.1.4.3 Refrigerant layout hole numbers

In order to ensure the heat transfer effect inside the horizontal falling-film evaporator, it was necessary to set a reasonable numbers of liquid distribution holes to ensure the liquid film outside the heat exchange tube can keep a continuous and uniform flow state. Since the influence of liquid hole numbers on the distribution characteristics of liquid film outside the tube was mainly reflected in the axial direction, the distribution of axial liquid film thickness was emphatically discussed. The axial liquid film thickness distribution of 90° week of tube and total heat transfer coefficient with liquid hole numbers of 7, 9, 11 and 14 for the single tube was described in Fig. 15 and Fig. 16. The liquid hole numbers of 7, 9, 11 and 14 corresponded hole center distance of 18 mm, 14 mm , 10 mm and 8 mm respectively.

The fluctuation of tube axial liquid film thickness distribution gradually reduced and liquid film thickness difference between peak and trough decreased when fluid hole numbers increased from 9 to 14. It was because the increase of liquid hole numbers resulted in the decrease of single-hole flow at a constant liquid spray density and liquid column transverse distance, which was more conducive to liquid film flow and spread out along the tube axial to improve the continuity and uniformity of liquid film distribution outside the tube. When fluid hole numbers decreased to 7, the axial liquid film thickness distribution changed a lot and the liquid film thickness of 0 (“dry up” area) appeared. Due to the sparse number of liquid hole, the tube axial liquid can’t spread out into a complete continuous liquid film and the situation was not conducive to heat exchange. What’s more, it indicated that the settings of liquid hole numbers do have a critical value.

As can be seen from Fig. 16, the total heat transfer coefficient presented an upward trend with the larger liquid distribution hole numbers. Because the more dense axial liquid distribution hole was more conducive to form a complete liquid film along the tube axial, improving the overall heat transfer. This rule was especially obvious at small Reynolds number because the “dry up” area outside the tube was more likely to appear to affect the

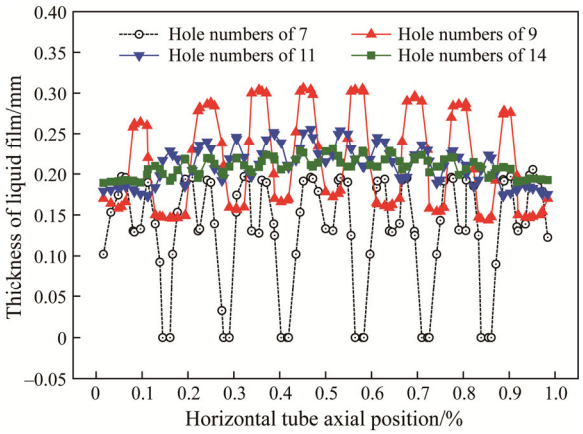

Fig. 15 Axial distribution of liquid film thickness with different layout hole numbers

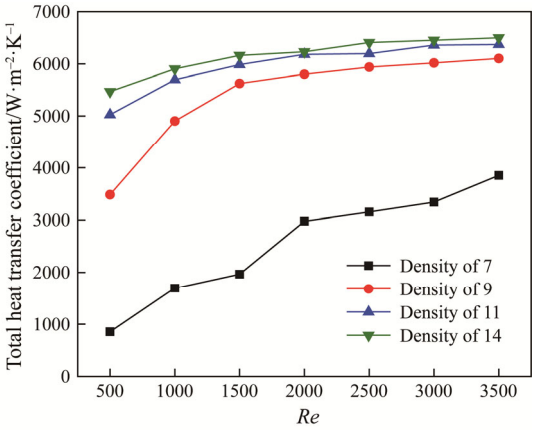

Fig. 16 Effects of different layout hole numbers on total heat transfer coefficient

heat transfer. The total heat transfer coefficients of hole numbers of 9, 11 and 14 were 134.36%, 117.13% and 141.71% higher than that of hole number of 7 respectively, which was caused by the "dry up" area at too few holes case. The changing extent of total heat transfer coefficient by Reynolds number at liquid hole number of 14 was less than the other three working conditions. It was because the large enough liquid hole number can guarantee the tube axial liquid forming a complete continuous film to reach a relatively ideal heat transfer effect. However, the inhibitory effect on heat transfer gradually revealed with further increase of refrigerant spray amount due to the thickening and local accumulation of liquid film. Therefore, the densely arranged liquid holes on heat transfer enhancement were not obvious at a large Reynolds number.

3.2 Horizontal tube falling-film evaporator

3.2.1 Analysis of flow field distribution characteristics

The characteristics of flow field distribution in falling film evaporator were studied in this paper. The velocity vector diagram and local magnification diagram at y=0 section and x=0 section of shell side of horizontal falling-film evaporator were shown in Fig. 17. The refrigerant flowed vertically down from liquid distribution hole and formed film on the heat exchange tube bundle. Part of refrigerant evaporated into a gaseous state and flowed out from air passage between tube bundles. Then gas refrigerant gathered on both sides of evaporator and flowed upward to steam outlets at the top. Part of refrigerant liquid which was not fully vaporized flowed out through the lower liquid outlet. Therefore, the fluid was relatively concentrated and the flow velocity was relatively high near the refrigerant distributor and outlet of upper and lower outlets, while the flow velocity was relatively low and evenly distributed in the falling-film flow area of heat exchange tube bundle. As can be seen from the local magnification of velocity vector, the refrigerant flow rate was lower on the lower position of heat exchange tube wall with the falling film flow evaporation between tube bundles went on. For a single heat exchange tube, the refrigerant flow in the lower half was less than that in the upper half. The velocity vector of local area in the lower half of vertical fifth row heat exchange tube was not covered, indicating the "dry up" area appeared.

As the gas generated by phase change of refrigerant would flow out through the channel between tube bundles and flow upward from both sides of evaporator, it will inevitably cause the disturbance of liquid film flow outside the tube. At the same time, part of refrigerant liquid would be carried into the steam outlet, leading to liquid suction in the refrigeration system. As can be seen from the local magnification of velocity vector, the upper tube bundle near the liquid distributor was more susceptible to the updraft gas. Therefore, baffle can be set at the air passage on both sides of evaporator to reduce the risk of liquid suction in the actual falling film evaporator design and manufacture, which was applied in patent of Dingel et al. [31].

3.2.2 Analysis of temperature distribution characteristics

At present, the temperature distribution characteristics of horizontal falling film evaporation process were mainly focused on the circumferential temperature distribution of heat exchange tube based on the

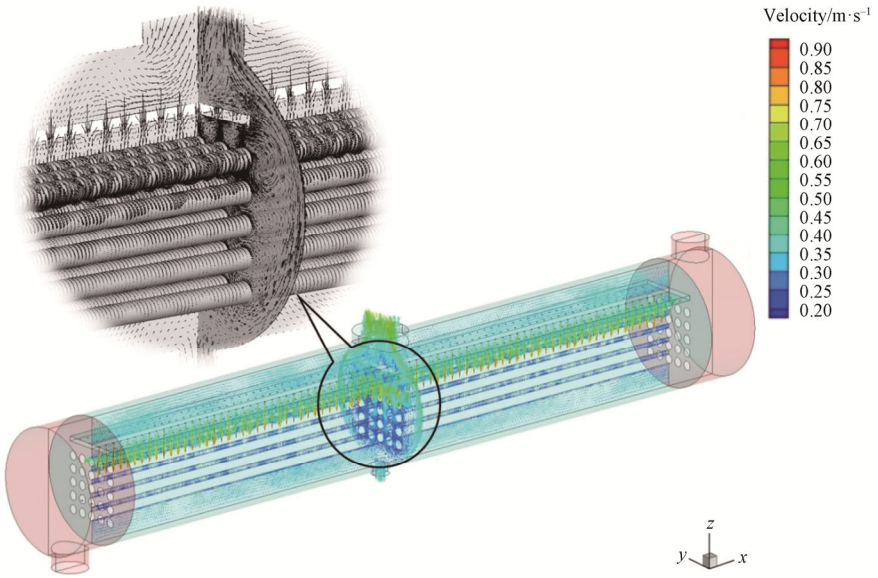

Fig. 17 Vector diagram of fluid velocity at shell side

two-dimensional model, while the temperature distribution in the tube axial direction and horizontal row tube and vertical row tube direction were rarely studied. Contour of temperature distribution on the tube wall and y=0 section under different spray densities at the same time was depicted in Fig. 18. The refrigerant falling film flow and evaporation absorbed heat, making the heat exchange tube wall temperature decrease steadily and uniformly along the tube axial direction. In addition, the tube wall temperature presented a gradually rising trend along the vertical downward direction (negative z-axis direction). It was because the partial refrigerant evaporated after passing upper heat exchange tube and the flow mass through the lower heat exchange tube decreased, reducing the heat transfer effect of lower heat exchange tube. Compared with the vertical direction, there was less difference in tube wall temperature between tubes in the same row along the horizontal direction (y-axis direction). For a single heat exchange tube, it can be observed that the upper tube outer wall temperature was significantly lower than that of the lower wall, especially for the first row of heat exchange tube, because the upper tube wall was directly impacted by the falling film flow of refrigerant. What's more, the direct impact of refrigerant on the lower tube of heat exchange was gradually weakened and the phenomena "Upper cold and lower hot" of the single heat exchange tube was gradually reduced.

In addition, the high-temperature area on the heat exchange tube outer wall moved towards the inlet direction and gradually decreased with the larger refrigerant spray density, corresponding to the decrease of tube outlet water temperature. The increase of spray density can lead to the increase of refrigerant flow rate to the lower tube path and occurrence of "Upper cold and lower hot" in the single heat exchange tube wall temperature. As the refrigerant continuously evaporated to absorb heat, the shell side of heat exchanger can always maintain the evaporation temperature.

Compared with the distribution law and variation trend of tube wall temperature, it was more valuable for practical engineering to explore the fluid temperature change in the tube. The temperature distribution contours of fluid in x=0 section, y=0 section and in the tube of falling film evaporator at Γ_L=0.09 kg·m^{-1}·s^{-1} were shown in Fig. 19. The fluid temperature along the tube axis gradually decreased and the upper tube temperature was obviously lower than that of lower tube temperature. In addition, the overall change trend of fluid temperature was similar to the above discussion of tube wall temperature.

In order to further explore the distribution law of fluid temperature on the tube path, the temperature at different positions of each heat exchange tube was calculated, shown in Fig. 20. The curves in the figure from bottom to top were vertical tube rows from 1 to 5. The tube fluid average temperature decreased gradually along the axial direction and it dropped faster in the first third area of tube path, and then the downward trend tended to be stable. From the vertical comparison of heat exchanger tubes, it can be found that the fluid temperature in the upper heat exchanger tube was higher than that in the lower part and the temperature difference in the fluid flow direction was getting larger and larger. From the horizontal comparison of heat exchange tubes, it indicated that the change law and value of fluid temperature were relatively close in the same horizontal row heat exchange tubes and the fluid temperature in the

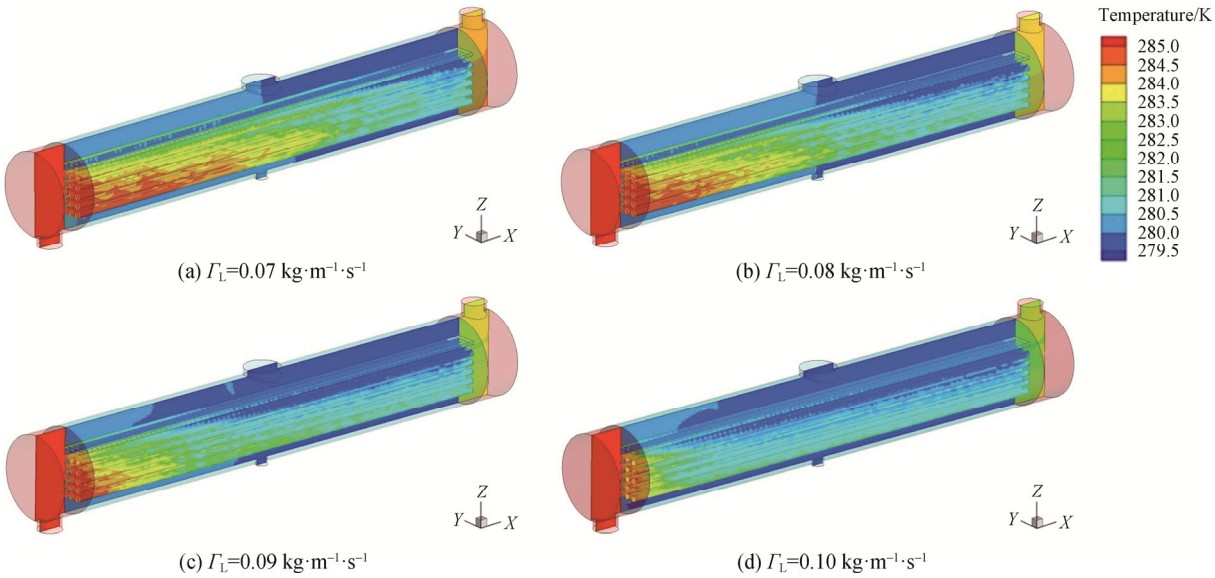

Fig. 18 Contour of temperature distribution on the tube wall under different spray densities at the same time

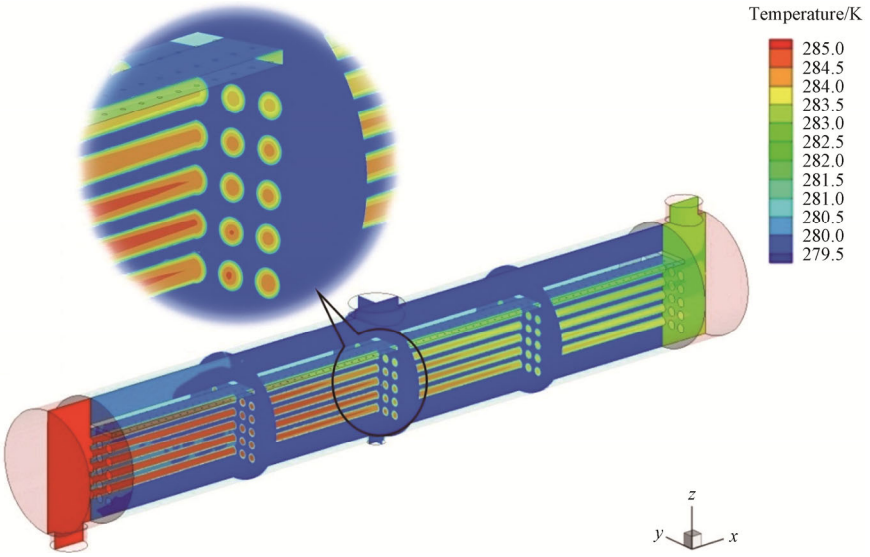

Fig. 19 Temperature distribution contour of fluid in the tube at Γ_L=0.09 kg·m^{-1}·s^{-1}

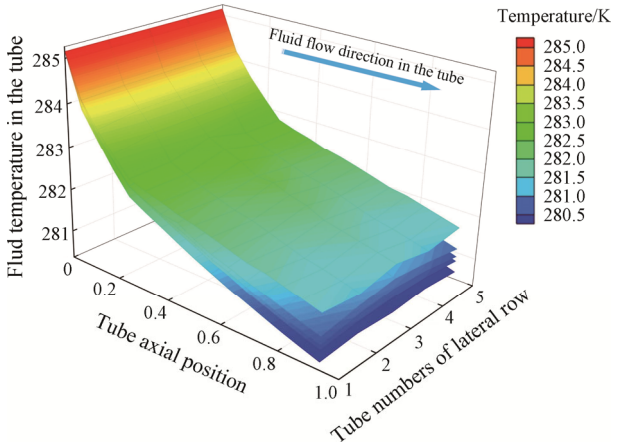

Fig. 20 The distribution of fluid temperature in different heat exchange tubes

middle heat exchange tube was slightly higher than that in other heat exchange tubes. This was because the rising vapor flow on both sides of heat exchange tubes caused the disturbance of liquid film on the tube outer wall, enhancing the heat transfer to some extent.

3.2.3 Analysis of heat transfer coefficient distribution characteristics

The distribution law of heat transfer coefficient of each tube bundle in the whole evaporator internal space was shown in Fig. 21. As the refrigerant falling film evaporated, the local heat transfer coefficient on the heat exchange tube surface in the vertical direction (*z*-axis direction) presented a downward trend and the downward trend was more obvious with the smaller spray density, which was consistent with temperature distribution law. The local heat transfer coefficient of upper heat exchanger near the refrigerant dispenser decreased gradually along the tube circumference, while it presented a regular fluctuation along the axial tube. The local heat transfer coefficient was high in the impact area directly below each liquid distribution hole, while the local liquid film thickness was large in the liquid film accumulation area between the liquid distribution holes, resulting in the increase of thermal resistance and decrease of local heat transfer coefficient, which was consistent with the previous analysis. However, since the lower heat exchange tubes was not sprayed directly by the liquid distribution hole, the refrigerant flow was random to some extent because of air flow disturbance and the local heat transfer coefficient distribution no longer strictly presented the above characteristics.

When the refrigerant spray density was small, the local heat transfer coefficient on the lower heat exchange tube surface was significantly reduced. Moreover, some areas were even lower than 200 W·m^{-2}·K^{-1} and these areas correspond to the "dry up" area on the heat exchange tube wall without velocity vector coverage, resulting in a decrease in the effective heat transfer area and a sharp deterioration of heat transfer. It was worth noting that more "dry up" area appeared in the middle of evaporator tube bundle. This was because the refrigerant gas phase outlet was set in the middle and the gas flow was relatively dense, causing the damage to the liquid film on the lower heat exchange tube surface with small refrigerant flow mass. The local heat transfer coefficient on the heat exchange tube surface increased gradually with the increase of spray density and the "dry up" area decreased gradually.

The total heat transfer coefficient distribution of heat exchange tube in the falling film evaporator at spray density of Γ_L=0.09 kg·m^{-1}·s^{-1} was depicted in Fig. 22. The total heat transfer coefficient of all heat exchangers

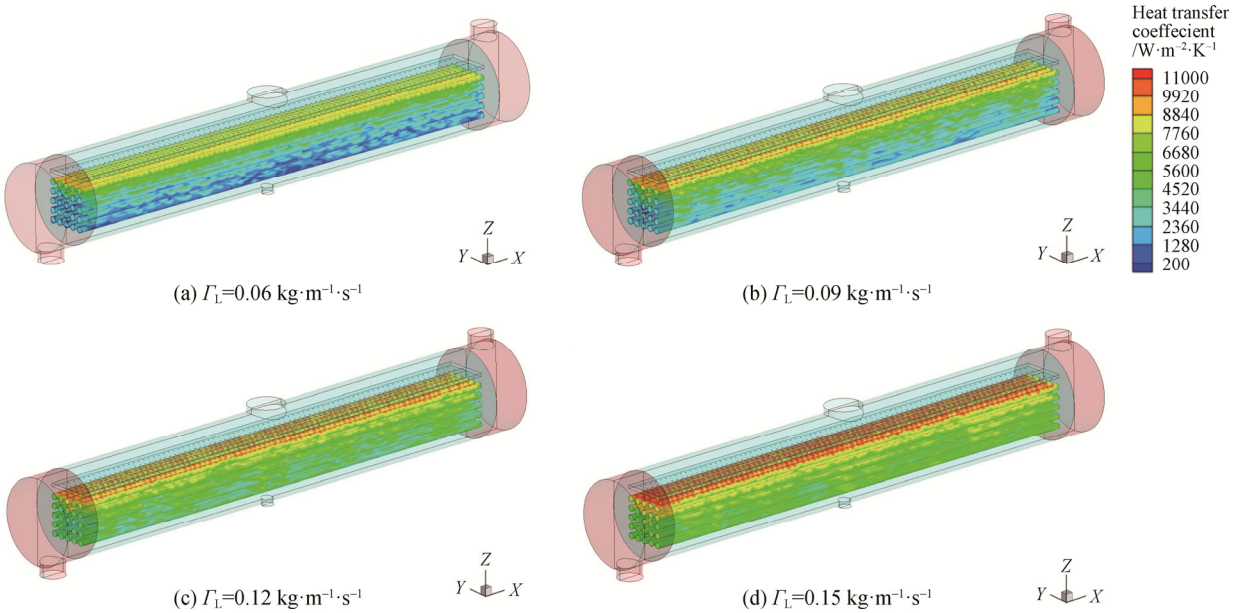

Fig. 21 Contour of heat transfer coefficient on the tube wall under different spray densities

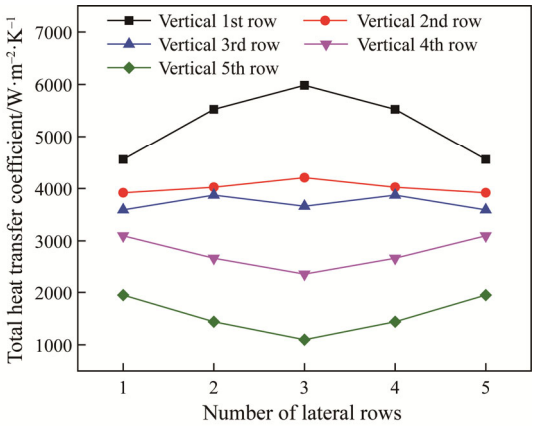

Fig. 22 Total heat transfer coefficient of different tubes

in the vertical direction presented a downward trend and the average total heat transfer coefficient of the second, third, fourth and fifth vertical heat exchangers was 74.52%, 71.10%, 53.15% and 30.10% of the first row respectively. The heat transfer coefficient of middle upper tube was significantly higher and presented "middle high and both sides low" characteristics for the horizontal tubes. It was because the upper tubes on both sides were near the liquid flow channel and part of the refrigerant can be taken away by rising steam, leading to the decrease of actual refrigerant flow rate and total heat transfer coefficient. The heat transfer coefficient of lower tube presented "middle low and both sides high" characteristic. This was because the updraft on both sides dominated the disturbance of liquid film flow on the heat exchange tube surface at this time, enhancing the heat transfer effect.

5. Conclusions

In this paper, the three-dimensional numerical models of refrigerant (R410A) falling film flow evaporation outside the horizontal single tube and inside the evaporator were established and the relevant simulation was carried out. For falling film flow evaporation outside the horizontal single tube, the results showed that the total heat transfer coefficient was low and increased with the larger spray density and evaporation temperature. The thickness of liquid film outside the tube decreased gradually with the increase of tube diameter, and the total heat transfer coefficient of small tube diameter was significantly greater than that of the large tube diameter, especially at a lower spray density. The total heat transfer coefficient presented an increasing trend with the increase of liquid distribution height and density. In addition, the fluctuation of tube axial liquid film thickness distribution and the difference of liquid film thickness at the crest and trough gradually decreased with larger liquid distribution density.

For the falling film flow evaporation in the evaporator, the results indicated that refrigerant in the upper and lower outlet was relatively concentrated and the flow rate was relatively high, leading to carry part of liquid refrigerant into the vapor outlet in the refrigeration system. The temperature of tube wall and fluid in the tube presented a gradually rising trend in the vertical downward direction, while the temperature of tube wall within the same horizontal and transverse row had little difference. The high-temperature zone on the outer wall of heat exchange tube moved towards the inlet and

gradually decreased, and the outlet temperature of water in the tube also gradually decreased with the increase of refrigerant spray density. The local heat transfer coefficient of heat exchanger tube in the vertical direction presented a downward trend, which was more obvious with the smaller spray density. For horizontal tube rows, the heat transfer coefficient of heat exchange tube was obviously higher located in the middle of upper tube row and both sides of lower tube row. The influence law of different parameters on the evaporation of falling film flow outside the horizontal tube was explored, providing a theoretical guidance for developing the falling film evaporator with higher energy efficiency to realize energy saving and emission reduction.

Acknowledgements

This study is financially supported by National Natural Science Foundation of China (No. 52006031) and international cooperation project of China Manned Space Program (6903001173).

References

[1] Jiao Y.H., Horizontal falling-film evaporator spray uniformity analysis and small mass flow falling-film numerical simulation. Huazhong University of Science and Technology, Wuhan, China, 2012.

[2] People Republic of China. China statistical yearbook. China statistical publisher, 2015.

[3] Ribatski G., Jacobi A.M., Falling-film evaporation on horizontal tubes-a critical review. International Journal of Refrigeration, 2005, 28(5): 635–653.

[4] Wang X.F., He M.G., Zhang Y., Numerical simulation of the liquid flowing outside the rube of the horizontal-tube falling film evaporator. Journal of Engineering Thermophysics, 2008, 29(8): 1347–1350.

[5] He M.G., Wang X.F., Zhang Y., et al., Study of flow regime and numerical simulation of film thickness on horizontal-tube falling film evaporator. Journal of Thermal Science and Technology, 2007, 6(4): 319–325.

[6] Qiu Q., Zhu X., Mu L., et al., Numerical study of falling film thickness over fully wetted horizontal round tube. International Journal of Heat and Mass Transfer, 2015, 84: 893–897.

[7] Yang L., Wang W., Zhou J.Q., Numerical simulation of the structural optimization of tube bundles in horizontal-tube falling film evaporators. Journal of Shandong Jianzhu University, 2012, 27(2): 193–197.

[8] Yang L., Liu Y., Yang Y., et al., Microscopic mechanisms of heat transfer in horizontal-tube falling film evaporation. Desalination, 2016, 394: 64–71.

[9] Yang L.P., Zhou Z.Y., Li H.Y., Numerical simulation of the heat transfer characteristics of the falling-film vaporization outside a horizontal tube. Journal of Engineering for Thermal Energy and Power, 2017, 32(10): 24–28.

[10] Jafar F., Thorpe G., Turan Ö., Liquid film falling on horizontal plain cylinders: numerical study of heat transfer in unsaturated porous media. International Journal for Computational Methods in Engineering Science & Mechanics, 2014, 15(2): 101–109.

[11] Zhou Y., Cai Z., Ning Z., et al., Numerical simulation of double-phase coupled heat transfer process of horizontal-tube falling film evaporation. Applied Thermal Engineering, 2017, 118: 33–40.

[12] Gstoehl D., Roques J.F., Crisinel P., et al., Measurement of falling film thickness around a horizontal tube using a laser measurement technique. Heat Transfer Engineering, 2004, 25(8): 28–34.

[13] He M.G., Fan H.L., Wang X.F., et al., Experimental study and numerical simulation on falling film thickness outside a horizontal tube. Journal of Xi'an Jiaotong University, 2010, 44(9): 1–5.

[14] Xu L., Wang S.C., Wang Y.X., et al., Heat-transfer film coefficients outside tube of falling film horizontal-tube evaporator. Journal of Chemical Industry and Engineering, 2004, 55(1): 19–24.

[15] Xu L., Wang S.C., Wang Y.X., et al., Flowing state of liquid films over horizontal tubes and its influences on heat-transfer characteristics. Journal of Chemical Industry and Engineering, 2002, 53(6): 555–559.

[16] Parken W.H.J., Heat transfer to thin water films on horizontal tubes. Thesis, Rutgers University, 1975.

[17] Parken W.H., Fletcher L.S., Heat transfer in thin liquid films flowing over horizontal tubes. Begel House Inc, 1982, 4: 415–420.

[18] Parken W.H., Fletcher L.S., Han J.C., et al., Heat transfer through falling film evaporation and boiling on horizontal tubes. Journal of Heat Transfer, 1990, 112: 3(3): 744–750.

[19] Jin B.H., Zhao C.Y., Liu Q.X., et al., Experimental study on R410A evaporation with horizontal smooth single tube falling film. 2016, http://www.paper.edu.cn.

[20] Ouldhadda D., Idrissi A.I., Asbik M., Heat transfer in non-Newtonian falling liquid film on a horizontal circular cylinder. Heat and Mass Transfer, 2002, 38(7–8): 713–721.

[21] Zhang N., Shao X., Simulation on the inner flow of different distributors in the falling film evaporator with horizontal tubes. Energy Conservation, 2012, 31(5): 19–24.

[22] Hasanpour B., Irandoost M.S., Hassani M. Numerical investigation of saturated upward flow boiling of water in a vertical tube using VOF model: effect of different boundary conditions. Heat and Mass Transfer, 2018, 54:

1925–1936.

[23] Lee W.H., A pressure iteration scheme for two-phase modeling. Technical Report LA-UR 79-975, Los Alamos Scientific Laboratory, Los Alamos, New Mexico, 1979.

[24] Mohammad B., Abas R., Ali A.R., Numerical simulation of bubble behavior in subcooled flow boilingunder velocity and temperature gradient. Nuclear Engineering and Design, 2015, 293: 238–248.

[25] Jeongmin L., Lucas E.O.N., Seunghyun L., Experimental and computational investigation on two-phase flow and heat transfer of highly subcooled flow boiling in vertical upflow. International Journal of Heat and Mass Transfer, 2019, 136: 1199–1216.

[26] Jin P.H., Zhao C.Y., Liu J.X., et al., An experimental study of falling film evaporation outside a horizontal plain tube with R410. China Science and Technology Papers online, 2016, http://www.paper.edu.cn.

[27] Killion J.D., Garimella S., Gravity-driven flow of liquid films and droplets in horizontal tube banks. International Journal of Refrigeration, 2003, 26(5): 516–526.

[28] Killion J.D., Garimella S., Pendant droplet motion for absorption on horizontal tube banks. International Journal of Heat and Mass Transfer, 2004, 47(19): 4403–4414.

[29] Killion J.D., Garimella S., Simulation of pendant droplets and falling films in horizontal tube absorbers. Journal of Heat Transfer, 2004, 126(6): 597–607.

[30] Ouyang X.P., Qiu X.S., Jiang F., Experimental investigation on the falling film evaporation of R404A outside a horizontal tube. Journal of Refrigeration, 2014, 35(1): 77–81.

[31] Dingel B.E., Larson J.W., Flow distributor and baffle system for a falling film evaporator. US, Patent No. 6830099.